Applied Energy 368 (2024) 123557

Contents lists available at ScienceDirect

Applied Energy

journal homepage: www.elsevier.com/locate/apenergy

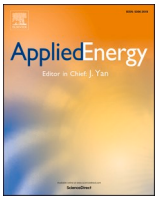

Development of one-step synthesized SO_4^{2-}/ZrO_2-fly ash (SZ@FA) solid acid catalysts for energy-efficient sorbent regeneration in CO_2 capture processes.

Yingjie Niu [a,1], Ting Li [a,1], Ali Hassan Bhatti [b], Jiaqi Qu [a], Xin Zhou [a], Li Luo [a], Francesco Barzagli [c,*], Chao'en Li [d], Rui Zhang [a,*]

[a] College of Chemical Engineering, Xiangtan University, Xiangtan, Hunan 411105, PR China
[b] University of Science and Technology, 217 Gajeong-ro Yuseong-gu, Daejeon 34113, South Korea
[c] National Research Council, ICCOM Institute, via Madonna del Piano 10, 50019 Sesto F.no, Florence, Italy
[d] CSIRO Energy, 71 Normanby Road, Clayton North, VIC 3169, Australia

HIGHLIGHTS

- Fly ash functionalized with SO_4^{2-}/ZrO_2 (SZ@FA) to catalyze CCUS desorption process
- MEA regeneration at 88 °C with SZ@FA is more efficient than the non-catalyzed system
- Decrease in energy consumption by up to 45.4% compared to non-catalyzed system

ARTICLE INFO

Keywords:
Carbon capture
Solid catalyst
SO_4^{2-}/ZrO_2
Fly ash
Heat duty

ABSTRACT

The use of solid acid catalysts for sorbent regeneration is an emerging approach to improve the energy efficiency of CO_2 capture processes. In this study, fly ash (FA), an industrial byproduct rich in acid/base sites, was chosen as a support material for the solid acid SO_4^{2-}/ZrO_2 (SZ) in the preparation of SZ@FA composite catalysts. Three catalysts with different mass ratios between SZ and FA were synthesized and evaluated in the regeneration process at 88 °C of a CO_2-saturated MEA solution. Their desorption performance, expressed as CO_2 desorption rate, amount of CO_2 desorbed, and heat duty, was then compared with that obtained with unmodified FA, ZrO_2, and in the absence of catalysts (blank), under identical operating conditions. Compared to the uncatalyzed system, the SZ@FA composite catalysts showed significantly better desorption performance. In particular, SZ@FA-1/2 provided the highest values of desorption rate and cyclic capacity while reducing energy consumption by 45.4% compared to the blank system. It also demonstrated stability over 20 consecutive absorption-desorption cycles. Comparison with other reported catalysts highlighted the high performance of SZ@FA-1/2, particularly in terms of relative heat duty reduction, positioning it as a cost-effective and environmentally friendly choice for post-combustion capture applications.

1. Introduction

The extensive use of fossil fuels across various industrial sectors results in the constant emission of large amounts of carbon dioxide (CO_2) into the atmosphere [1]. This causes significant environmental impacts, including worsening the greenhouse effect, rising sea levels, and more frequent extreme weather events [1,2]. Industries such as oil refineries [3], pulp and paper industries [4], steel mills [5], coal gasification facilities [6], and fossil fuel power plants [7] are key contributors to CO_2 emissions.

The development of Post-Combustion Capture (PCC) technologies, which selectively capture CO_2 from flue gases originating from industrial emissions (typically containing 10–15% CO_2) [8], is now considered essential to mitigate the increase in atmospheric CO_2 [9,10], as well as developing technologies to safely (and permanently) store the captured CO_2, such as storing it as gas hydrates in the ocean [11,12].

Chemical sorption based on aqueous solutions of amines is considered to be the most suitable and mature approach for PCC, characterized

* Corresponding authors.
E-mail addresses: francesco.barzagli@iccom.cnr.it (F. Barzagli), ruizhang@xtu.edu.cn (R. Zhang).
[1] Yingjie Niu and Ting Li contributed equally to this work and are the co-first authors.

https://doi.org/10.1016/j.apenergy.2024.123557
Received 28 November 2023; Received in revised form 26 April 2024; Accepted 22 May 2024
Available online 29 May 2024

by rapid and reversible reactions between CO_2 and low-cost and readily available amines [13]. However, the significant energy requirement for sorbent regeneration has so far limited the wide deployment of this technology [14].

Several strategies have been explored to address this problem, including the development of efficient amine blends [15,16], biphasic solvents [17,18], catalytic CO_2 desorption [19,20], and so on. The total energy requirements for solvent regeneration in the CO_2 capture process typically consist of three parts, as shown in **Eq. 1**. These components include the sensible heat (Q_{sen}), needed to elevate the temperature of the absorber to the required level for desorption, the latent heat of evaporation (Q_{vap,H_2O}), required for evaporation of the water in the solvent, and the desorption heat (Q_{des,CO_2}), necessary to break the chemical bonds for CO_2 release (desorption) [21].

$$Q_{red} = Q_{sen} + Q_{vap,H_2O} + Q_{des,CO_2} \quad (1)$$

Conventional amine-based CO_2 capture technology typically requires a high temperature (above 120 °C) during the desorption process to decompose the species formed during absorption (amine carbamate, protonated amines, bicarbonate and carbonate ions) and regenerate the sorbent. Ethanolamine (MEA) is the most commonly used amine for this process [22], and its desorption stage accounts for over 70% of the total energy cost [23,24]. There are two main reasons for the high energy consumption in MEA regeneration. Firstly, the alkalinity of MEA is stronger than that of water, making the transfer of protons (H^+) from protonated MEA ($MEAH^+$) to H_2O challenging. As a result, additional energy is required to facilitate this proton transfer reaction. Secondly, the CO_2 desorption process is inherently endothermic, requiring an external energy source to proceed [25]. Shi et al. [26] proposed a two-step mechanism for CO_2 desorption from MEA, which involves the decomposition of MEA carbamate ($MEACOO^-$) and the deprotonation process of $MEAH^+$, as shown in **Eqs. 2–3**. Both reactions are endothermic.

$$MEACOO^- + H_3O^+ \leftrightarrow Zwitterion \leftrightarrow MEA + H_2O + CO_2\uparrow \quad (2)$$

$$MEAH^+ + H_2O \leftrightarrow MEA + H_3O^+ \quad (3)$$

In recent years, the possibility of using solid acid catalysts (SAC) to assist amine regeneration at lower temperatures has been explored with increasing interest. SACs can provide Brønsted (B) and Lewis (L) acid sites that facilitate the reactions shown in **Eqs. 2–3**, significantly reducing the energy consumption for CO_2 desorption [27,28].

In this context, sulfated metal oxide catalysts (e.g., SO_4^{2-}/ZrO_2, SO_4^{2-}/TiO_2, etc.) are known to be acidic, stable, easy to synthesize, and environmentally safe, but their use is limited due to the rapid deactivation of catalytic activity and low specific surface area [29]. To address these issues, researchers suggest combining them with porous materials to create composite catalysts. Liang et al. [30] investigated the performance of several $SO_4^{2-}/ZrO_2/\gamma\text{-}Al_2O_3$ composite catalysts in the desorption of CO_2-loaded MEA solutions, and they found that the heat duty was reduced by 17.3–36.9% and the cyclic capacity increased by 11.3–33.9% compared to the system without catalyst. The same group also explored the catalytic activity of SO_4^{2-}/ZrO_2 supported on MCM-41 with the addition of Fe_2O_3 (10 wt%), finding an increased desorption rate and cyclic capacity by 54.7% and 51.8%, respectively, while reducing thermal duty by 39.4% [31].

Other research groups have independently developed SO_4^{2-}/ZrO_2-based composite catalysts with various support materials, such as SBA-15 [32], HSZM-5 [33], and SiO_2 [34], all demonstrating excellent performance in CO_2-loaded MEA solutions desorption. However, it's important to note that these support materials can be costly and environmentally damaging due to their synthetic production methods. Therefore, the development of efficient, cost-effective, and environmentally safe support materials is essential for advancing the application of SACs for PCC.

Fly ash (FA) is a solid waste byproduct derived from power plants, primarily composed of SiO_2, Al_2O_3, and Fe_2O_3. FA has specific characteristics such as bulk density, particle size, porosity, surface area, stability, and low cost, making it an excellent precursor for the synthesis of porous adsorbent materials [35], and support for catalysts [36].

These properties, together with the logistical advantage of using FA directly where it is produced, have led fly ash to be considered for various CCUS processes, such as in adsorption for CO_2 capture [37,38], catalysis for CO_2 utilization [39] or direct CO_2 storage through mineralization [40]. Owing to its intrinsic acidic characteristics, FA has also been recently evaluated as a solid acid catalyst for sorbent regeneration in PCC processes [41,42]. The observed performances, related to the desorption of MEA solutions, show that FA is a more effective catalyst than other SACs studied so far, reducing the heat duty by 38–42% compared to the uncatalyzed system. However, further research is needed to confirm and fully understand the potential of FA in this area.

Motivated by these findings, the present study aims to harness the advantages of the solid SO_4^{2-}/ZrO_2 superacid by combining it with low-cost FA support to develop a higher-performance composite catalyst for promoting CO_2 desorption.

Three new SZ@FA acid-base dual-functional composite catalysts were prepared by combining SO_4^{2-}/ZrO_2 and FA in different molar ratios (1:1, 1:2, and 2:1). Several characterization methods were used to analyze their physicochemical properties. Subsequently, their catalytic performance in regenerating CO_2-loaded MEA solutions at a temperature of 88 °C was experimentally evaluated by measuring heat duty, CO_2 desorption rate, and cyclic capacity. The stability of these new catalysts was also assessed through twenty consecutive CO_2 absorption/desorption experiments. Additionally, the desorption performance of these composite catalysts was compared with that of other SZ-based catalysts (with varying carriers) under identical operating conditions. Finally, we propose a plausible mechanism for the SZ@FA-catalyzed desorption.

2. Material and methods

2.1. Material

CO_2 (99.999%) and N_2 (99.9%) were acquired from Hunan Zhongtai Hongyuan Gas Co. Ltd. Monoethanolamine (MEA, 99%) was supplied by Shanghai Macklin Biochemical Co. Ltd. Fly ash (FA) was purchased from Lvmingyuan Environmental Protection Material Factory. ZrO_2 (99.99%) and $Zr(SO_4)_2{\cdot}4H_2O$(99.99%) were supplied by Beijing Innochem Technology Co. Ltd. and Aladdin Biochemical Technology Co. Ltd., respectively. Hydrochloric acid (HCl, 36–38%) was obtained from Hunan Huihong Reagent Co. Ltd. All the chemicals were used without further purification.

2.2. Preparation of the SZ@FA catalyst

One-step method was used in this work to synthesize the SO_4^{2-}/ZrO_2@Fly ash (SZ@FA) catalyst. $Zr(SO_4)_2{\cdot}4H_2O$ and FA were dispersed in deionized water and stirred in an oil bath (80 °C) for 24 h; the resulting precipitate was subsequently washed three times with deionized water, transferred to an oven, and dried at 120 °C for 24 h. The dried solid was placed into a mortar, ground into a fine powder and then heated at 500 °C (heating rate of 5 °C/min) in a muffle furnace for 4 h to obtain the calcined SZ@FA catalysts with different mass ratios of ZrO_2: FA (1/2, 1/1 and 2/1), which were labeled as SZ@FA-1/2, SZ@FA-1/1 and SZ@FA-2/1, respectively.

2.3. Catalyst characterization techniques

The textural parameters, acid types and strength of acidity and basicity of each catalyst tested were comprehensively characterized using different techniques, described in detail in **Section S1** of the ***Supporting Information***.

2.4. Sorbent regeneration experiments

To evaluate CO_2 desorption with or without different catalysts, it is necessary to have a CO_2-saturated amine solution as a starting point. In our study, an aqueous solution of 5 M MEA was saturated using a flow of pure CO_2 (200 mL/min) for 8 h at a constant temperature of 40°. At the end of the absorption, the CO_2 loading of the saturated sorbent, defined as the ratio of the moles of CO_2 absorbed to the moles of amine in solution (mol CO_2/mol amine), was measured by titration with HCl (1 M), yielding a value of 0.535.

The desorption process was studied following a procedure developed and validated in our laboratory [19]. The instrumentation used for these experiments is shown in **Fig. S1** in the ***Supporting Information***. All desorption experiments used the same starting sorbent, i.e., saturated solution of MEA, with CO_2 loading = 0.535. The sorbent was desorbed in a batch reactor (a 500 mL glass three-necked flask) placed in an oil bath, equipped with a magnetic stirrer and temperature controller. In each experiment, 2.0 g of the catalyst under investigation was added to 200 mL of the loaded MEA solution and heated to the desorption temperature (T = 88 °C) for 1 h, at room pressure. Experiments were conducted using both the three designed SZ@FA composite catalysts and the unmodified FA and ZrO_2 supports. To verify the effectivity of the catalysts compared with the uncatalyzed system, desorption experiments without the addition of any solid (blank system) were also performed under the same experimental conditions. A constant flow of N_2 (500 mL/min) was blown into the reactor to facilitate the release of CO_2. The reactor was fitted with a condenser set at a temperature of 0 °C, a drying tube, and a sulfuric acid bottle to reduce losses of water and amine. A CozIR-100 infrared CO_2 detector (GSS Ltd.) was connected at the end of the desorption unit to measure the concentration of CO_2 in the outlet gas mixture. Each experiment was repeated three times, and the deviation from the mean measured value was always in the range of 0.5–1.5%. From the measured CO_2 concentration values, the CO_2 desorption rate, the total amount of CO_2 released (i.e. the cyclic capacity), and the CO_2 loading of the solution during the regeneration process were calculated. During the experiments, the electrical energy consumed was recorded by an energy meter (Zhejiang Tepsung Electric Co., Ltd.) and used to calculate the heat duty, i.e. thermal energy required to release each mole of CO_2 from the saturated solution. It's important to note that the calculation of the heat duty using this method is greatly affected by the equipment used. Therefore, the comparison of these values is only meaningful when obtained with the same experimental setup, as was done in this study. To make our findings more significant and comparable to other studies in the literature, we also included the relative heat duty, which is the percentage ratio between the heat duty measured with the catalyst and that measured for the MEA reference solution (blank) under the same operating conditions. Details regarding the calculation of the parameters used to evaluate desorption performance are provided in **Section S2** of the ***Supporting Information***.

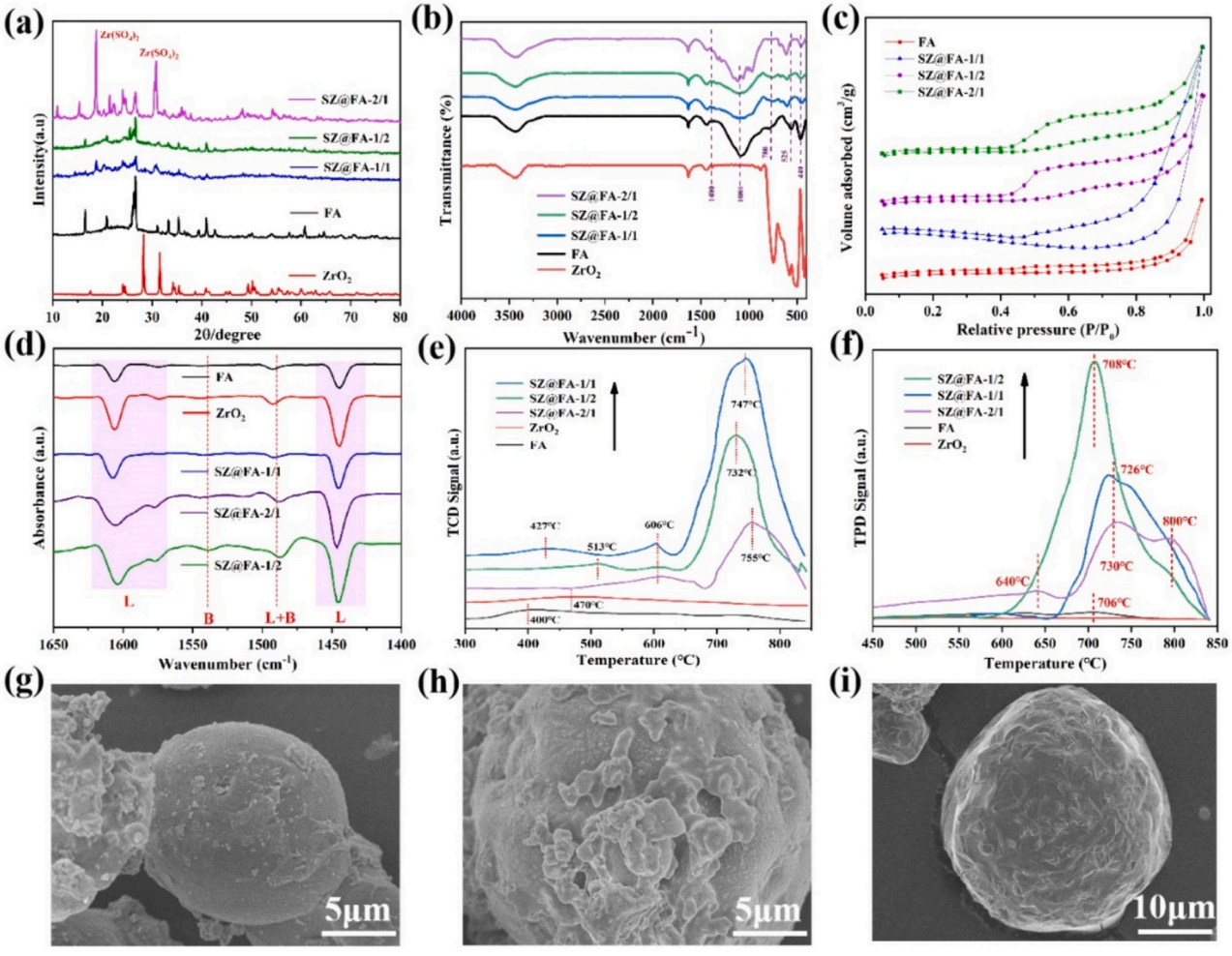

Fig. 1. Spectroscopic characterization of the different catalysts used by: (a) XRD (b) FT-IR (c) N_2-adsorption-desorption (d) Py-IR (e) NH_3-TPD and (f) CO_2-TPD. SEM images of (g) SZ@FA-1/2, (h) SZ@FA-1/1 and (i) SZ@FA-2/1.

3. Results and discussions

3.1. Characterization of the used catalysts

The X-ray diffraction (XRD) spectra for both FA and SZ@FA series catalysts are shown in Fig. 1a. The patterns reveal that, with the introduction of Zr into the single FA, the SZ@FA-2/1 showed distinct diffraction peaks at 18.7° and 31.5°, indicating that ZrO_2 was successfully loaded onto the FA substrate. According to phase analysis, ZrO_2 in SZ@FA-2/1 mainly existed in the form of $Zr(SO_4)_2$ crystal phase. The content of Zr in the prepared SZ@FA series catalysts was quantified by the inductively coupled plasma optical emission spectroscopy (ICP-OES), and the results showed that SZ@FA-1/2, SZ@FA-1/1 and SZ@FA-2/1 contained 16.29%, 20.73% and 24.08% of Zr, respectively, with an increasing Zr content as the mass ratio between ZrO_2 and FA increased. At the same time, it was observed that SZ@FA-1/1 and SZ@FA-1/2 had smaller diffraction peaks, which could be due to the reduced ZrO_2 content in the catalyst or the microcrystals being too small to be detected by XRD. Overall, the feature peaks of FA and SZ@FA catalysts were similar, indicating that the addition of FA carriers did not change the crystal composition of SO_4^{2-}/ZrO_2. The corresponding feature peaks of the SZ@FA series catalysts showed a slight decrease in intensity, which can be attributed to the interaction between FA and ZrO_2. This suggests that ZrO_2 was dispersed on the surface of the FA carrier successfully and even infiltrated into the individual pore channels of FA, ultimately resulting in a decrease in the feature peaks. Scanning electron microscope (SEM) images of the SZ@FA series catalysts are shown in **Fig. 1g, h** and **i**. The images show that SZ is uniformly dispersed on the FA surface, and the SZ content increases with the increasing SZ abundance in the SZ@FA composite; in particular, SZ almost covered the FA surface in the SZ@FA-2/1 catalyst. The FT-IR spectra of the different catalysts are shown in Fig. 1b, revealing distinct changes in the spectral bands of the SZ@FA series catalysts within the 1400 and 1040 cm^{-1}. These changes correspond to the asymmetric and symmetric stretching vibrations of the S═O double bond, partially ionized S═O double bond, and S—O single bond in the sulfate. Moreover, the shifts in the spectral band at 1080 cm^{-1} suggest the formation of Zr-O-Si bonds in the SZ@FA catalyst. In addition, changes were observed at characteristic peaks associated with ZrO_2 in the 440–525 cm^{-1} range. This suggests that some of the ZrO_2 exists in the form of dispersed clusters on the SiO_2 of the fly ash. The collective findings from FT-IR and XRD analyses provide corroborating evidence for the successful synthesis of SZ@FA catalysts.

The catalysts' specific surface area and pore structure were further examined through BET characterization tests. The N_2 absorption-desorption curves are depicted in Fig. 1c. The specific pore structure and values for the specific surface area of the various catalysts are summarized in Table 1. When SO_4^{2-}/ZrO_2 (SZ) was introduced, a significant change in the hysteresis loop profile of the SZ@FA catalyst was observed for relative pressure values in the range 0.4–1.0. This might be due to the surface loading of SZ on the parent FA. As the proportion of SZ in the catalyst increased, the specific surface area gradually decreased, following the order: FA (2.99 m^2/g) > SZ@FA-1/2 (2.11 m^2/g) > SZ@FA-1/1 (2.03 m^2/g) > SZ@FA-2/1 (0.53 m^2/g). It is noteworthy that the average pore size of the SZ@FA series catalysts consistently appeared smaller than that of unmodified FA catalysts, suggesting that the introduction of SZ led to pore clogging in the FA. However, within a certain range, increasing the percentage of SZ may widen the original channel structure and increase the pore size [33]: for example, SZ@FA-2/1 had a larger average pore size (12.61 nm) compared to SZ@FA-1/2 (7.41 nm). A simultaneous reduction in the microporous and mesoporous diameters of the SZ@FA catalysts was also observed in the pore size distribution. The results are consistent with the XRD patterns, indicating that the added SZ may mainly be situated within the FA channels or uniformly dispersed on the inner surface of the FA. In general, these outcomes indicate that the SO_4^{2-}/ZrO_2 components have been successfully integrated into the parent FA.

Table 1
Textural parameters of the used catalysts.

Catalyst	BET Surface Area (m^2/g)			Pore volume (cm^3/g)	Pore size (nm)
	Micropore	Mesoporous	Total		
FA	2.24	0.75	2.99	0.002	15.39
SZ@FA-2/1	0.23	0.30	0.53	0.001	12.61
SZ@FA-1/1	1.38	0.65	2.03	0.003	12.86
SZ@FA-1/2	1.62	0.49	2.11	0.003	7.41

The Py-IR technique was used to identify Brønsted (B) and Lewis (L) acids in the catalysts, as shown in Fig. 1d. The Py-IR spectra showed four characteristic peaks at 1445, 1490, 1547, and 1600 cm^{-1}. The results indicated that the SZ@FA catalysts contained more Lewis acid sites (LAS) and fewer Brønsted acid sites (BAS). Among all the catalysts, SZ@FA-1/2 had the strongest characteristic peak of B acid. Specific values for B and L acidity in the prepared catalysts can be found in Table 2. Generally, the introduction of SZ increases the number of both B and L acid sites compared to the starting FA for all composite catalysts. The highest value of total acid sites (TAS) was achieved by SZ@FA-1/2. The B/L ratio of SZ@FA-2/1 was 0.076 mmol/g, which is lower than that of unmodified FA (0.087 mmol/g). This decrease might be due to the strong exchange of H^+ protons on the surface of Zr^{4+} and FA, along with the interaction of Zr^{4+} ions with the protons of the SiAl-OH group, which transforms from a strong B acid center into a strong L acid during calcination. In contrast, the B/L ratios of SZ@FA-1/1 and SZ@FA-1/2 were higher, 0.124 and 0.109 mmol/g, respectively. This suggest that only a few Zr^{4+} ions in the material can interact with the SiAl-OH group, while most of the Zr^{4+} ions interact with the non-acidic terminal silanol group (Si-OH) of FA.

As shown in Fig. 1e, the relative contents of strong, medium-strong, and weak acids were determined through NH_3-TPD (ammonia temperature-programmed desorption) characterization. Notably, there were no characteristic peaks below 200 °C, indicating that all catalysts were almost free of weak acid centers. However, characteristic peaks of varying intensities appeared in the temperature range of 400–800 °C. FA and ZrO_2 catalysts appeared as strong acids with small peak areas at 400 °C and 470 °C, respectively. In contrast, the SZ@FA series of prepared catalysts predominantly featured distinctive super-strong acid characteristic peaks near 750 °C, with peak intensities following the order: SZ@FA-1/1 > SZ@FA-1/2 > SZ@FA-2/1. Quantitative values of the acidic sites (mmol/g) are shown in Table 2. The data indicate that the introduction of SO_4^{2-}/ZrO_2 significantly increased the number of strong acidic sites and the overall acid content in the FA-based catalysts. Therefore, the synthesized SZ@FA series catalysts are expected to facilitate proton transfer in the desorption process and enhance the CO_2 desorption rate during sorbent regeneration.

The desorption peak temperature and peak area in the CO_2 programmed thermal desorption (CO_2-TPD) profile are shown in Fig. 1f, reflecting the strength and number of basic sites on the sample surface, respectively. The corresponding data are summarized in Table 2. In the CO_2-TPD profile, the absence of a CO_2 desorption peak for ZrO_2 suggests a potential lack of alkaline centers on its surface. The FA sample had a narrower peak at 706 °C, indicating the presence of fewer strong alkaline sites. However, upon loading SO_4^{2-}/ZrO_2 onto the FA sample's surface, both the position and area of the peaks were shifted to higher values, signifying the generation of stronger basic sites. As shown in Fig. 1f, SZ@FA-1/1 exhibited a broader peak at 726 °C, indicating the emergence of stronger basic centers. The SZ@FA-2/1 sample displayed one weaker and two broader CO_2 desorption peaks at 640 °C, 730 °C, and 800 °C, respectively, resulting from the chemical adsorption of CO_2 over weaker and stronger basic centers. Finally, SZ@FA-1/2 produced a very strong peak at 708 °C, with the corresponding alkaline intensity

Table 2
Acid type and the strength of acidity and basicity of the catalyst.

Catalyst	Acid type by Py-IR (mmol/g)				Acidity strength by NH_3-TPD (mmol/g)				Basicity strength by CO_2-TPD (mmol/g)			
	BAS	LAS	TAS	B/L	Weak	Medium	Strong	Total	Weak	Medium	Strong	Total
ZrO_2	0.199	2.137	2.336	0.093	0.049	0.029	0.085	0.163	0.004	0.007	0.008	0.019
FA	0.119	1.362	1.481	0.087	0.023	0.039	0.146	0.208	0.002	0.006	0.035	0.043
SZ@FA-2/1	0.275	3.622	3.897	0.076	0.008	0.011	0.385	0.404	0.045	0.089	0.362	0.496
SZ@FA-1/1	0.223	1.793	2.016	0.124	0.045	0.102	1.027	1.134	0.020	0.082	0.314	0.416
SZ@FA-1/2	0.418	3.838	4.256	0.109	0.020	0.033	0.615	0.668	0.045	0.083	0.510	0.638

reaching 0.510 mmol/g, as a result of the interaction between SO_4^{2-}/ZrO_2 and FA. The results highlight that the basicity strength of SZ@FA composites is higher with a higher proportion of FA, underscoring the significance of the FA proportion in the catalyst.

3.2. Catalytic CO_2 desorption performance of SZ@FA

Experiments to assess the CO_2 desorption performance of the catalysts were conducted at a temperature of 88 °C from a CO_2-saturated solution of aqueous MEA (loading = 0.535), following the procedure described in Section 2.4. The results are summarized in Fig. 2.

Fig. 2a shows the changes in CO_2 instantaneous desorption rate as the desorption proceeds for the different catalytic and non-catalytic systems. In general, CO_2 began to be released after about 5 min (at a temperature of about 65 °C), and the desorption rate increased rapidly before decreasing significantly after reaching the maximum value. All catalysts outperformed the non-catalytic system in CO_2 desorption rate, with the maximum values obtained decreasing in the order FA > SZ@FA-1/2 > SZ@FA-1/1 > SZ@FA-2/1 > ZrO_2 > uncatalyzed system. SZ@FA-1/2 showed a significant advantage in promoting the CO_2 release rate during the first few minutes of heating compared to the other catalysts. This suggests that FA in the SZ@FA series plays a crucial role, and a lower proportion of SZ enhances the catalytic performance of FA. Fig. 2b, which reports the changes in CO_2 loading during desorption, shows that for the same amount of time, the use of SZ@FA-1/2 ensures a greater decrease in CO_2 loading (and thus greater sorbent regeneration), promoting the desorption of a larger amount of CO_2, as also depicted in Fig. 2c. Typically, the CO_2-rich amine solution remains in the desorber for a short time, so a faster desorption rate with a higher desorbed CO_2 amount can result in a lower energy requirement for releasing CO_2, which is beneficial for reducing operating costs.

Table 3 provides a summary of the average CO_2 desorption rate, cyclic capacity, and heat duty of different catalytic systems at 25 min. The results show that the SZ@FA composite catalysts improve the average desorption rate and cyclic capacity by 11.3–78.3% and 11.4–77.7%, respectively, while reducing the heat duty by 13.0–45.4%

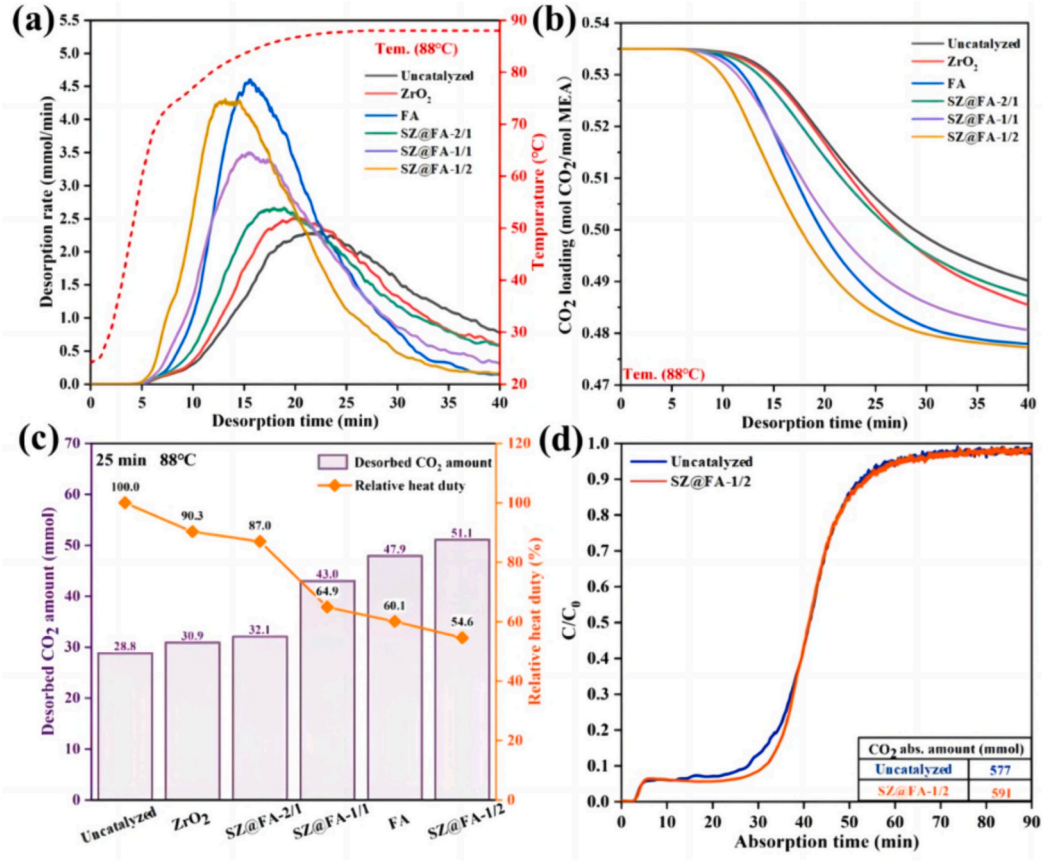

Fig. 2. CO_2 desorption performance with or without catalyst: (a) CO_2 desorption rate and (b) CO_2 loading as a function of time; (c) relative heat duty and desorbed CO_2 after 25 min of desorption (catalyst quantity: 0.50 g, amine solution volume: 200 mL, desorption temperature: 88 °C). (d) Evaluation of the effect of the SZ@FA-1/2 catalyst on CO_2 absorption performance.

Table 3
Average CO_2 desorption rate, cyclic capacity, and heat duty for 5 M MEA solution with/without catalyst (des. T: 88 °C; des. Time: 25 min).

Catalyst	Average desorption rate ($*10^{-2}$ mol/min)	Cyclic capacity ($*10^{-2}$ mol)	Heat duty (kJ/mol)
Blank	1.15	28.78	4002.92
ZrO_2	1.24	30.89	3614.63
FA	1.91	47.85	2407.52
SZ@FA-2/1	1.28	32.06	3482.54
SZ@FA-1/1	1.72	42.99	2597.90
SZ@FA-1/2	2.05	51.14	2185.59

compared to the non-catalytic system. Among these, SZ@FA-1/2 showed the best catalytic desorption performance.

Furthermore, Figs. 2a-2c indicate that the content of FA carrier in the SZ@FA series catalysts plays a pivotal role in the catalytic CO_2 desorption process, and loading a lower amount of SO_4^{2-}/ZrO_2 on the FA carrier can enhance the catalytic activity of FA. This is likely because the SZ@FA-1/2 has the highest specific surface area (Table 1) and the lowest SZ content (16.29% according to ICP-OES). The better dispersion of SZ in SZ@FA-1/2, compared to SZ@FA-1/1 and SZ@FA-2/1 where SZ content is higher, allows the catalyst's active sites to better interact with species in the CO_2-rich solution, leading to improved catalytic performance. With a view to the continuous use of the sorbent in the absorption and desorption cycles, the effect of the SZ@FA-1/2 catalyst on the CO_2 absorption performance was evaluated (Fig. 2d**):** the amount of CO_2 absorbed after 90 min with the addition of the SZ@FA-1/2 catalyst was 591 mmol, approximatively 2.4% higher than in the system without the catalyst. This further indicates that the SZ@FA-1/2 catalyst not only enhances the desorption process but also has no inhibiting effect on the absorption process. Finally, to assess a possible effect of the catalyst toward amine stability, MEA solutions desorbed with SZ@FA-1/2 and without catalyst (blank) were analyzed by ^{13}C NMR spectroscopy: the spectra obtained showed no change in the type of species in solution.

3.3. *Catalytic stability of SZ@FA-1/2*

The of the SZ@FA-1/2 catalyst was evaluated through 20 consecutive absorption-desorption cycles. Fig. 3a depicts the amount of desorbed CO_2 and the heat duty measured during all 20 consecutive desorption, that were performed over a period of 25 min. In the initial 13 tests, the heat duty increased and the amount of desorbed CO_2 decreased, indicating that the activity sites of SZ@FA-1/2 had decreased due to the adsorption of free CO_2 during recycling. However, from the 14th test onwards, the desorbed CO_2 and the heat duty stabilized, suggesting a relatively stable catalytic activity of SZ@FA-1/2. Comparison of the FT-IR and XRD spectra of the SZ@FA-1/2 catalyst before and after 20 recycling tests reveals no significant changes (**Fig. 3b** and **c**), which means that the structure of the SZ@FA-1/2 catalyst remains almost unchanged, ensuring a relatively stable catalytic activity over time.

1.1. *Comparison of catalytic CO_2 desorption performance*

To evaluate the potential of our SZ@FA composite catalysts for CO_2 desorption, we compared their relative heat duty with other SZ-based catalysts that have already been proven effective for catalyzed sorbent regeneration, as reported in the literature [30–34]. These catalysts have

Table 4
Comparison of heat duty for different SO_4^{2-}/ZrO_2^- based catalysts.

Catalyst	Desorption temperature (°C)	Relative heat duty (%)	Ref.
SZ@FA-1/2	88	54.6	This study
SZ@FA-1/1		64.9	
SZ@FA-2/1		87.0	
SZ@HZSM-5	98	69–82	[33]
SZ@SiO_2	97	63.5–77.1	[34]
SZ@MCM-41		75.5–81.1	
SZ@MCM-41-Fe_2O_3	97	60.6–72.3	[31]
SZ@SBA-15	98	73.4–81.0	[32]
SZ@γ-Al_2O_3	98	63.1–75.1	[30]

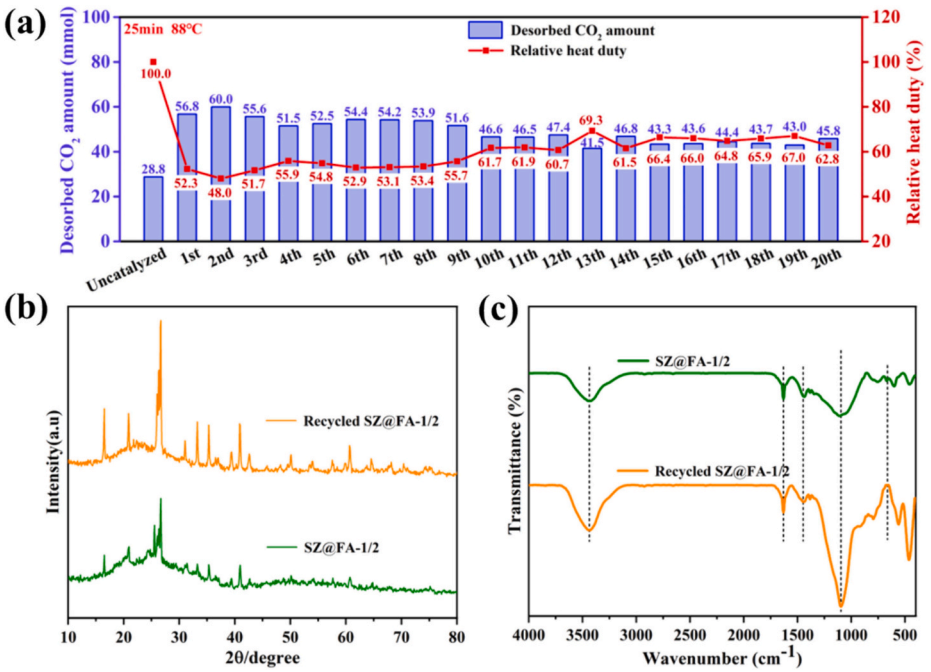

Fig. 3. (a) Relative heat duty and amount of desorbed CO_2 measured after 25 min for all 20 stability tests; comparison of (b) XRD and (c) FT-IR spectra of fresh and recycled SZ@FA-1/2.

different catalytic supports and their relative heat duty values, presented in Table 4, were measured referring to conventional aqueous MEA 5 M without any catalyst. The comparison highlights that SZ@FA-1/2 outperforms other reported catalysts in CO_2 desorption, yielding the lowest relative heat duty (54.6% compared to uncatalyzed MEA). It is worth noting that all of the reported catalyst supports, i.e. HZSM-5, SiO_2, MCM-41, SBA-15, and γ-Al_2O_3, are synthesized using chemical methods, which, in addition to the unavoidable negative environmental impact, adds cost to the overall CO_2 capture process. In this context, the use of solid waste FA to prepare the catalyst is not only beneficial for environmental protection (solid waste treatment) but also provides a way to expand its application in energy-efficient (and cost-effective) CO_2 capture.

1.2. *Analysis of the catalytic mechanism for CO_2 desorption*

The main challenges for the CO_2 desorption are the deprotonation of $MEAH^+$ and the decomposition of $MEACOO^-$ (**Eqs. 2 and 3**): both reactions are endothermic and contribute largely to heat consumption in the solvent regeneration process. The key to improving these two processes is to allow the H^+ protons to be transferred more easily, and this can be achieved with a solid acid catalyst that can provide LAS and BAS for the MEA and CO_2 release process. The prepared SZ@FA catalysts are shown to have more LAS and BAS than FA, which allows SZ@FA to enhance the CO_2 desorption process.

Firstly, the metal oxides were found to be able to indirectly generate BAS in aqueous solution, as shown in **Eq. 4**. Strong interactions between oxides and water molecules can undergo chemisorption, leading to the formation of hydroxyl groups (i.e., surface-bound OH groups) and consequently in the formation of BAS [43,44]. According to Khatri et al. [36], ZrO_2 is attached to the FA surface via Si-O-Zr bonds, and SO_4^{2-} binds to Zr atoms to form a bidentate chelating ligand. Secondly, sulfate bound to water molecules on the surface can generate BAS, Zr^{4+} can provide LAS, and Si-OH or Si-O-Zr-OH groups on the FA surface may also act as sources of BAS. Moreover, interconversion between LAS and BAS can take place, as shown in Fig. 5.

Based on previous studies, possible mechanisms of SZ@FA catalysts to promote CO_2 desorption from CO_2-rich amine solutions were explored. On one hand, the carbamate ion $MEACOO^-$, the main product of the reaction between MEA and CO_2, is basic. The FA catalyst itself contains a significant number of metal oxides, along with loaded ZrO_2 that form anions in alkaline solutions. These anionic groups serve as Lewis basic, capable of directly interacting with the proton of $MEAH^+$, thereby facilitating the deprotonation process (**Eq. 5**). In addition, ZrO_2 can be converted to zirconate ion ($HZrO_3^-$) in the alkaline environment [45], providing a low-temperature reaction path for proton transfer from $MEAH^+$ to $MEACOO^-$ (**Eqs. 5–7**).

$$MO + H_2O \rightarrow MO \bullet H_2O \rightarrow MOH \bullet OH \tag{4}$$

$$MEAH^+ + HZrO_3^- \leftrightarrow MEA + H_2ZrO_3 \tag{5}$$

$$H_2ZrO_3 + H_2O \leftrightarrow HZrO_3^- + H_3O^+ \tag{6}$$

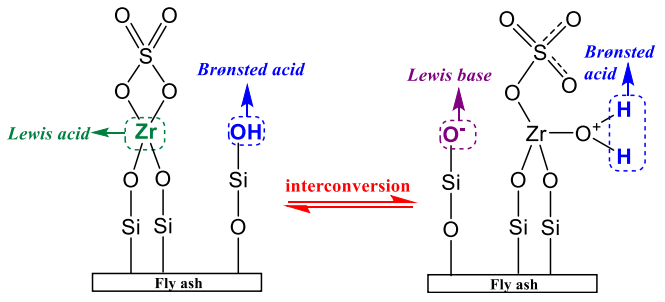

Fig. 5. Schematic representation of acid-base sites of SZ@FA catalysts.

$$MEACOO^- + H_2ZrO_3 \leftrightarrow MEACOOH + HZrO_3^- \tag{7}$$

On the other hand, the BAS and LAS on the catalyst surface promote the decomposition of $MEACOO^-$, and the reaction takes place mainly through the following steps: (1) The H^+ released from BAS in solution and provided by the products of **Eqs. 6 and 7** participate in the decomposition process of $MEACOO^-$; (2) chemisorption occurred between the LAS on the catalyst surface and the $MEACOO^-$, and the unsaturated metal atoms (from Zr and FA) attacked the O atom; (3) H^+ is transferred from the O atom to the neighboring N atom through an isomerization process while the conjugate bond of the N atom is disrupted by the H^+ proton, transforming from sp^2 to sp^3 hybridization, and the C—N bond begins to stretch; (4) simultaneously, LAS attacks the N atom and further elongates the C—N bond, enhancing the CO_2 desorption process; (5) finally, the zwitterion ($MEAH^+COO^-$) decomposed into free MEA and CO_2 by breaking the C—N bond. In addition, the conjugated base (BAS^-) formed in step 1 can also accept the H^+ from the $MEAH^+$ to release free MEA (**Eqs. 8 and 9**).

$$MEACOO^- + H - BAS \leftrightarrow MEACOOH + BAS^- \tag{8}$$

$$MEAH^+ + BAS^- \leftrightarrow MEA + H - BAS \tag{9}$$

The recovered BAS-H can then participate in subsequent catalytic decomposition processes. Typically, this step is challenging to carry out without a catalyst and requires a significant amount of external heat; the addition of an acid catalyst to the reaction enhances the breakdown of the C—N bond by lowering the activation energy.

4. Conclusion

In this research, novel solid acid catalysts were devised to improve the regeneration of sorbents employed in CO_2 capture, aiming to diminish the overall energy demand of PCC processes. We synthesized three distinct SZ@FA composite catalysts by loading the SO_4^{2-}/ZrO_2 superacid on a fly ash (FA) support, in different ratios (2:1, 1:1, 1:2).

Their efficiency in catalyzing CO_2 desorption from a saturated aqueous solution of MEA heated to 88 °C was assessed experimentally by quantifying the CO_2 desorption rate, cyclic capacity, and heat duty. The findings revealed that all SZ@FA catalysts exhibited significantly superior desorption performance compared to both the non-catalyzed system (MEA without any added solids) and the utilization of unmodified ZrO_2 under identical operational conditions. Notably, the SZ@FA-1/2 catalyst yielded the best performance, showing the highest average CO_2 desorption rate, the highest cyclic capacity (78% greater than the blank), and most importantly, the lowest relative energy consumption, 45.4% lower than the uncatalyzed MEA reference system. The SZ@FA-1/2 catalyst was further investigated. Comparison with the relative heat duty of other catalysts reported in the literature showed its excellent performance in CO_2 desorption. In addition, its recyclability was demonstrated with twenty consecutive adsorption/desorption experiments, during which the catalyst maintained its activity. XRD and FT-IR analysis also confirmed that the catalyst structure did not change significantly after recycling, indicating good cyclic stability. Finally, a possible dual-site synergistic catalytic mechanism of the FA-based composite catalyst was proposed.

Our results highlight the potential of the SZ@FA-1/2 composite catalyst to reduce expenses associated with PCC processes due to its CO_2 desorption capabilities and use of fly ash, a cost-effective industrial by-product whose reuse instead of disposal offers environmental benefits. However, its implementation on an industrial scale will require validation on large-scale systems and a thorough cost-benefit assessment.

CRediT authorship contribution statement

Yingjie Niu: Writing – original draft, Methodology, Investigation. **Ting Li:** Writing – original draft, Methodology, Investigation. **Ali**

Hassan Bhatti: Methodology. **Jiaqi Qu:** Investigation. **Xin Zhou:** Investigation. **Li Luo:** Investigation. **Francesco Barzagli:** Writing – review & editing, Writing – original draft, Supervision, Methodology, Conceptualization. **Chao'en Li:** Supervision, Funding acquisition. **Rui Zhang:** Writing – review & editing, Writing – original draft, Supervision, Funding acquisition, Conceptualization.

Declaration of competing interest

The authors declare that they have no known competing financial interests or personal relationships that could have appeared to influence the work reported in this paper.

Data availability

No data was used for the research described in the article.

Acknowledgments

The work was supported by the National Natural Science Foundation of China (22008204), the Natural Science Foundation of Hunan Province (2023JJ30580), Research Start-up Foundation of Xiangtan University (21QDZ56). The authors thank the ICCOM Institute of the Italian National Research Council for the facilities and the financial support through the project PARCO2 (project code DCM.AD004.254).

Appendix A. Supplementary data

Supplementary data to this article can be found online at https://doi.org/10.1016/j.apenergy.2024.123557.

References

[1] Qureshi MF, Zheng J, Khandelwal H, Venkataraman P, Usadi A, Barckholtz TA, et al. Laboratory demonstration of the stability of CO_2 hydrates in deep-oceanic sediments. Chem Eng J 2022;432:134290. https://doi.org/10.1016/j.cej.2021.134290.

[2] Li L, Zhao N, Wei W, Sun Y. A review of research progress on CO_2 capture, storage, and utilization in Chinese Academy of Sciences. Fuel 2013;108:112–30. https://doi.org/10.1016/j.fuel.2011.08.022.

[3] Arvidsson M, Heyne S, Morandin M, Harvey S. Integration opportunities for substitute natural gas (SNG) production in an industrial process plant. Chem Eng Trans 2012;29:331–6. https://doi.org/10.3303/CET1229056.

[4] Onarheim K, Santos S, Kangas P, Hankalin V. Performance and costs of CCS in the pulp and paper industry part 1: performance of amine-based post-combustion CO_2 capture. Int J Greenhouse Gas Control 2017;59:58–73. https://doi.org/10.1016/j.ijggc.2017.02.008.

[5] Leeson D, Mac Dowell N, Shah N, Petit C, Fennell PS. A techno-economic analysis and systematic review of carbon capture and storage (CCS) applied to the iron and steel, cement, oil refining and pulp and paper industries, as well as other high purity sources. Int J Greenhouse Gas Control 2017;61:71–84. https://doi.org/10.1016/j.ijggc.2017.03.020.

[6] Bassani A, Bozzano G, Pirola C, Ranzi E, Pierucci S, Manenti F. Low impact methanol production from sulfur rich coal gasification. Energy Procedia 2017;105:4519–24. https://doi.org/10.1016/j.egypro.2017.03.970.

[7] Ahmed U, Kim C, Zahid U, Lee C-J, Han C. Integration of IGCC and methane reforming process for power generation with CO_2 capture. Chem Eng Process: Process Intensif 2017;111:14–24. https://doi.org/10.1016/j.cep.2016.10.020.

[8] Herzog H. A research program for promising retrofit technologies. MIT Symposium on Retrofitting of Coal-fired Power Plants for Carbon Capture: Citeseer; 2009.

[9] Xiao M, Liu H, Gao H, Olson W, Liang Z. CO_2 capture with hybrid absorbents of low viscosity imidazolium-based ionic liquids and amine. Appl Energy 2019;235:311–9. https://doi.org/10.1016/j.apenergy.2018.10.103.

[10] Zhang R, Liu R, Barzagli F, Sanku MG, Ce Li, Xiao M. CO_2 absorption in blended amine solvent: speciation, equilibrium solubility and excessive property. Chem Eng J 2023;466:143279. https://doi.org/10.1016/j.cej.2023.143279.

[11] Qureshi MF, Khandelwal H, Usadi A, Barckholtz TA, Mhadeshwar AB, Linga P. CO_2 hydrate stability in oceanic sediments under brine conditions. Energy 2022;256:124625. https://doi.org/10.1016/j.energy.2022.124625.

[12] Evaluating CO_2 hydrate kinetics in multi-layered sediments using experimental and machine learning approach: applicable to CO_2 sequestration. Energy 2024;290:129947. https://doi.org/10.1016/j.energy.2023.129947.

[13] Lai Q, Kong L, Gong W, Russell AG, Fan M. Low-energy-consumption and environmentally friendly CO_2 capture via blending alcohols into amine solution. Appl Energy 2019;254:113696. https://doi.org/10.1016/j.apenergy.2019.113696.

[14] Wu X, Fan H, Mao Y, Sharif M, Yu Y, Zhang Z, et al. Systematic study of an energy efficient MEA-based electrochemical CO_2 capture process: from mechanism to practical application. Appl Energy 2022;327:120014. https://doi.org/10.1016/j.apenergy.2022.120014.

[15] Zhang R, Li Y, He X, Niu Y, Ce Li, Amer MW, et al. Investigation of the improvement of the CO_2 capture performance of aqueous amine sorbents by switching from dual-amine to trio-amine systems. Sep Purif Technol 2023;316:123810. https://doi.org/10.1016/j.seppur.2023.123810.

[16] Zhang R, Liu H, Liu R, Niu Y, Yang L, Barzagli F, et al. Speciation and gas-liquid equilibrium study of CO_2 absorption in aqueous MEA-DEEA blends. Gas Sci Eng 2023;119:205135. https://doi.org/10.1016/j.jgsce.2023.205135.

[17] Zhou X, Shen Y, Liu F, Ye J, Wang X, Zhao J, et al. A novel dual-stage phase separation process for CO_2 absorption into a biphasic solvent with low energy penalty. Environ Sci Technol 2021;55:15313–22. https://doi.org/10.1021/acs.est.1c01622.

[18] Yu Y, Shen Y, Zhou X, Liu F, Zhang S, Lu S, et al. Relationship between tertiary amine's physical property and biphasic solvent's CO_2 absorption performance: quantum calculation and experimental demonstration. Chem Eng J 2022;428:131241. https://doi.org/10.1016/j.cej.2021.131241.

[19] Zhang R, Li Y, Zhang Y, Li T, Yang L, Ce Li, et al. Energy-saving effect of low-cost and environmentally friendly Sepiolite as an efficient catalyst carrier for CO_2 capture. ACS Sustainable Chem Eng 2023;11:4353–63. https://doi.org/10.1021/acssuschemeng.2c06739.

[20] Li T, Yu Q, Barzagli F, Ce Li, Che M, Zhang Z, et al. Energy efficient catalytic CO2 desorption: mechanism, technological progress and perspective. Carbon capture. Sci Technol 2023;6:100099. https://doi.org/10.1016/j.ccst.2023.100099.

[21] Oexmann J, Kather A. Minimising the regeneration heat duty of post-combustion CO2 capture by wet chemical absorption: the misguided focus on low heat of absorption solvents. Int J Greenhouse Gas Control 2010;4:36–43. https://doi.org/10.1016/j.ijggc.2009.09.010.

[22] Vinjarapu SHB, Neerup R, Larsen AH, Jørsboe JK, Villadsen SNB, Jensen S, et al. Results from pilot-scale CO_2 capture testing using 30 wt% MEA at a waste-to-energy facility: optimisation through parametric analysis. Appl Energy 2024;355:122193. https://doi.org/10.1016/j.apenergy.2023.122193.

[23] Feng B, Du M, Dennis TJ, Anthony K, Perumal MJ. Reduction of energy requirement of CO_2 desorption by adding acid into CO_2-loaded solvent. Energy Fuel 2010;24:213–9. https://doi.org/10.1021/ef900564x.

[24] Hu H, Fang M, Liu F, Wang T, Xia Z, Zhang W, et al. Novel alkanolamine-based biphasic solvent for CO_2 capture with low energy consumption and phase change mechanism analysis. Appl Energy 2022;324:119570. https://doi.org/10.1016/j.apenergy.2022.119570.

[25] Liang Z, Rongwong W, Liu H, Fu K, Gao H, Cao F, et al. Recent progress and new developments in post-combustion carbon-capture technology with amine based solvents. Int J Greenhouse Gas Control 2015;40:26–54. https://doi.org/10.1016/j.ijggc.2015.06.017.

[26] Shi H, Naami A, Idem R, Tontiwachwuthikul P. Catalytic and non catalytic solvent regeneration during absorption-based CO_2 capture with single and blended reactive amine solvents. Int J Greenhouse Gas Control 2014;26:39–50. https://doi.org/10.1016/j.ijggc.2014.04.007.

[27] Idem R., Shi H., Gelowitz D., Tontiwachwuthikul P. Catalytic method and apparatus for separating a gaseous component from an incoming gas stream. International Patent: WO2011120138A1,PCT/CA2011/000328; 06.10.2011.

[28] Liang Z, Yu F, Liu H, Rongwong W, Idem R, Tontiwachwuthikul P. Experimental study on the solvent regeneration of a CO_2-loaded MEA solution using single and hybrid solid acid catalysts. AIChE J 2016;62:753–65. https://doi.org/10.1002/aic.15073.

[29] Jin T, Yamaguchi T, Tanabe K. Mechanism of acidity generation on sulfur-promoted metal oxides. J Phys Chem 1986;90:4794–6. https://doi.org/10.1021/j100411a017.

[30] Zhang X, Hong J, Liu H, Luo X, Olson W, Tontiwachwuthikul P, et al. SO_4^{2-}/ZrO_2 supported on γ-Al_2O_3 as a catalyst for CO2 desorption from CO_2-loaded monoethanolamine solutions. AIChE J 2018;64:3988–4001. https://doi.org/10.1002/aic.16380.

[31] Zhang X, Zhu Z, Sun X, Yang J, Gao H, Huang Y, et al. Reducing energy penalty of CO_2 capture using Fe promoted SO_4^{2-}/ZrO_2/MCM-41 catalyst. Environ Sci Technol 2019;53:6094–102. https://doi.org/10.1021/acs.est.9b01901.

[32] Gao H, Huang Y, Zhang X, Bairq ZAS, Huang Y, Tontiwachwuthikul P, et al. Catalytic performance and mechanism of SO_4^{2-}/ZrO_2//SBA-15 catalyst for CO_2 desorption in CO_2-loaded monoethanolamine solution. Appl Energy 2020;259:114179. https://doi.org/10.1016/j.apenergy.2019.114179.

[33] Xing L, Wei K, Li Q, Wang R, Zhang S, Wang L. One-step synthesized SO_4^{2-}/ZrO_2-HZSM-5 solid acid catalyst for carbamate decomposition in CO_2 capture. Environ Sci Technol 2020;54:13944–52. https://doi.org/10.1021/acs.est.0c04946.

[34] Bairq ZAS, Gao H, Huang Y, Zhang H, Liang Z. Enhancing CO_2 desorption performance in rich MEA solution by addition of $SO_4^{2-}/ZrO_2/SiO_2$ bifunctional catalyst. Appl Energy 2019;252:113440. https://doi.org/10.1016/j.apenergy.2019.113440.

[35] Arenillas A, Smith KM, Drage TC, Snape CE. CO_2 capture using some fly ash-derived carbon materials. Fuel 2005;84:2204–10. https://doi.org/10.1016/j.fuel.2005.04.003.

[36] Khatri C, Mishra MK, Rani A. Synthesis and characterization of fly ash supported sulfated zirconia catalyst for benzylation reactions. Fuel Process Technol 2010;91:1288–95. https://doi.org/10.1016/j.fuproc.2010.04.011.

[37] Chandrasekar G, Son W-J, Ahn W-S. Synthesis of mesoporous materials SBA-15 and CMK-3 from fly ash and their application for CO_2 adsorption. J Porous Mater 2009;16:545–51. https://doi.org/10.1007/s10934-008-9231-x.

[38] Zgureva D, Boycheva S. Experimental and model investigations of CO_2 adsorption onto fly ash zeolite surface in dynamic conditions. Sustain Chem Pharm 2020;15:100222. https://doi.org/10.1016/j.scp.2020.100222.
[39] Dindi A, Quang DV, Vega LF, Nashef E, Abu-Zahra MRM. Applications of fly ash for CO_2 capture, utilization, and storage. J CO2 Util 2019;29:82–102. https://doi.org/10.1016/j.jcou.2018.11.011.
[40] Tamilselvi Dananjayan RR, Kandasamy P, Andimuthu R. Direct mineral carbonation of coal fly ash for CO_2 sequestration. J Clean Prod 2016;112:4173–82. https://doi.org/10.1016/j.jclepro.2015.05.145.
[41] Niu Y, Li T, Barzagli F, Li C, Amer MW, Zhang R. Fly ash as a cost-effective catalyst to promote sorbent regeneration for energy efficient CO_2 capture. Energy 2024;294:130890. https://doi.org/10.1016/j.energy.2024.130890.
[42] Bhatti AH, Waris M, Hussain I, Chougule SS, Pasupuleti KS, Kariim I, et al. Renaissance of fly ash as eco-friendly catalysts for rapid CO_2 release from amines. Carbon Capture Sci Technol 2024;11:100198. https://doi.org/10.1016/j.ccst.2024.100198.
[43] Bhatti UH, Shah AK, Kim JN, You JK, Choi SH, Lim DH, et al. Effects of transition metal oxide catalysts on MEA solvent regeneration for the post-combustion carbon capture process. ACS Sustainable Chem Eng 2017;5:5862–8. https://doi.org/10.1021/acssuschemeng.7b00604.
[44] Bhatti UH, Sivanesan D, Lim DH, Nam SC, Park S, Baek IH. Metal oxide catalyst-aided solvent regeneration: a promising method to economize post-combustion CO2 capture process. J Taiwan Inst Chem Eng 2018;93:150–7. https://doi.org/10.1016/j.jtice.2018.05.029.
[45] Yurdakul A, Gunkaya G, Dolekcekic E, Kavas T, Karasu B. Novel glass compositions for fiber drawing. Ceram Int 2015;41:13105–14. https://doi.org/10.1016/j.ceramint.2015.07.024.